Supporting Information

# Electric field induced reversible and irreversible photoluminescence responses in methylammonium lead iodide perovskite

Xiaofan Deng, Xiaoming Wen*, Cho Fai Jonathan Lau, Trevor Young, Jae Yun, Martin A. Green, Shujuan Huang and Anita W. Y. Ho-Baillie*

Australian Centre for Advanced Photovoltaics, School of Photovoltaic and Renewable Energy Engineering, University of New South Wales, Sydney, 2052, Australia

## Sample preparation

The substrate is 1cm$^2$ TEC8 FTO|glass (8Ω/□ sheet resistivity). The FTO layer was patterned by laser scribing and an electrical isolation test was performed to make sure the clear scribe isolated the two regions of FTO. Before fabrication of perovskite layer, the substrates were ultra-sonicated sequentially in (a) a 2% solution of cleaning detergent diluted in deionized water, (b) deionized water, (c) ethanol and (d) isopropanol before drying with clean dry air. The substrates were further exposed to UV-ozone for 20 min. The perovskite $CH_3NH_3PbI_3$ films were synthesized by the gas-assisted spin-coating method as reported in literature [1]. A 25μL 45wt% $CH_3NH_3PbI_3$ in DMF solution was prepared from $PbI_2$ and $CH_3NH_3PbI_3$ with a molar ratio of 1:1. The solution was spun at 6500rpm for 30s while 40psi nitrogen gas was blown over the film 2s after the spin-coating commenced for 10s. The films were then annealed at 100°C for 10 min before cooling to room temperature. Gold electrodes that are approximately 25nm were sputtered at the edge of the sample with masking of perovskite part to complete the sample.

## Fluorescence imaging and time-correlated single photon counting (TCSPC) measurements

Both the Fluorescence imaging and TCSPC measurements were conducted on a confocal laser scanning microscope (Leica SP5 WLL STED) with excitation at 488 nm from pulsed white light laser and repetition rate of 20 MHz. The power intensity is ~ 100 mW/cm$^2$. The 100× oil objective (n=1.4) was used and the imaging resolution is 1024×1024. A low scan speed of 100 Hz was used to reduce the noise. The experiment was undertaken at room temperature.

## Scanning Electron Microscopy (SEM) measurement

SEM imaging was carried out on FEI Nova NanoSEM 230 FESEM instrument with a 10 kV/10 nA beam voltage/current

### Energy-dispersive X-ray spectroscopy (EDS)

EDS mapping was carried out on the NanoSEM 230 using a Bruker SDD-EDS detector.

**X-ray diffraction (XRD) measurement**

XRD patterns of the sample was obtained by a PANalytical Xpert Materials Research diffractometer system with a Cu Kα radiation source ( $\lambda = 0.1541$ nm) operating at 45 kV and 40 mA.

The cross-sectional SEM image in Figure S1a shows the microstructure of FTO electrodes and perovskite layer. The gap between FTO electrodes is ~ 20 µm. The thickness of FTO electrodes and perovskite layers are ~ 700 nm and 300 nm, respectively. The resistivity of $CH_3NH_3PbI_3$ perovskite is ~ $10^7$ Ω·cm at room temperature[2]. By considering the dimension of perovskite bulk between FTO electrodes which is ~ 1 cm × 20 µm × 300 nm (width × length × thickness), the resistance can be estimated as ~$10^9$ Ω (the direction of electric field is in parallel of layer surface). This is obviously much larger than the total resistance of FTO and gold electrodes. The voltage applied on to the gold electrodes can be taken as the voltage across the perovskite between the FTO electrodes. Figure S1b shows the X-ray diffraction (XRD) patterns of perovskite layer on FTO electrodes, with main peaks at 14.06°, 28.41° and 31.84° corresponding to the (110), (120) and (220) planes of the tetragonal perovskite structure, respectively.[3, 4] The SEM image and EDS elemental mappings of the same area of a pristine sample show uniform distribution of perovskite both on the FTO and in between the FTO electrodes, see Figure S2.

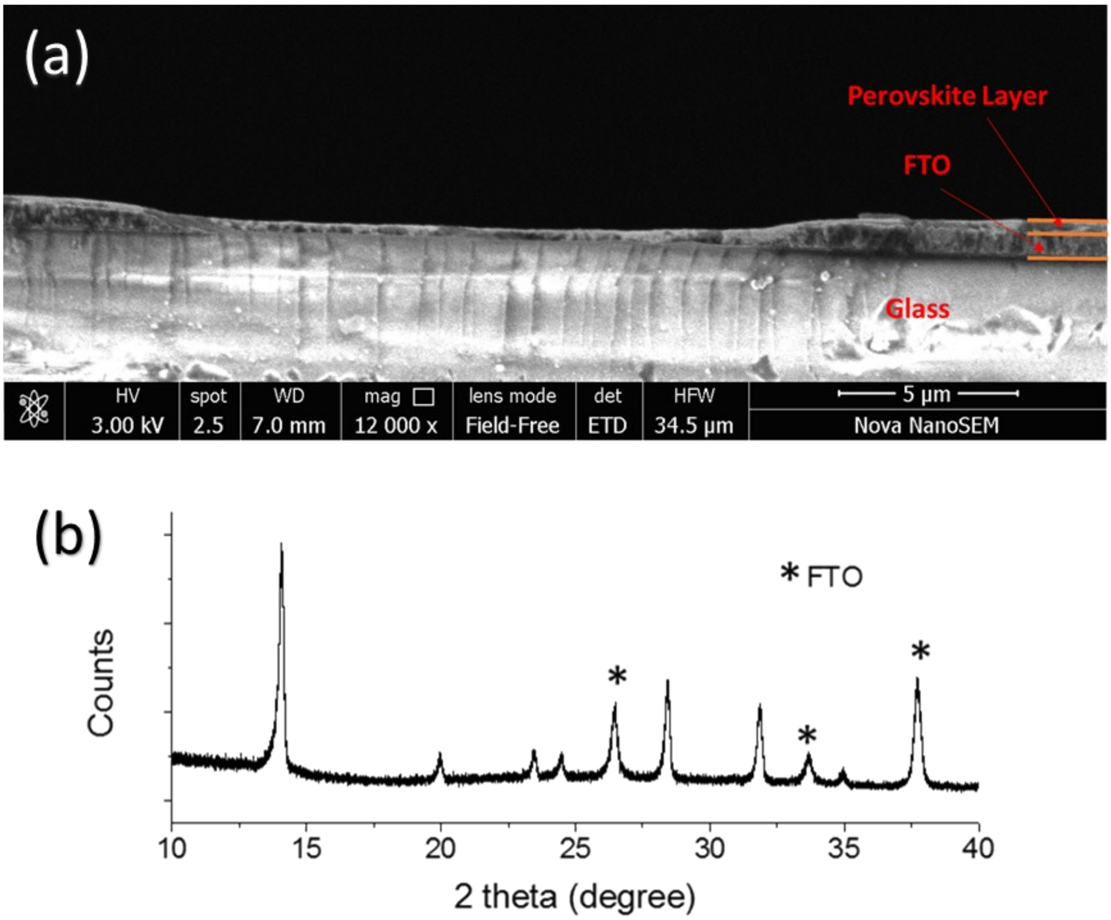

**Figure S1:** (a) Cross-section SEM image shows the microstructure of FTO electrodes and perovskite layer; (b) X-ray diffraction patterns for perovskite layer on FTO electrodes

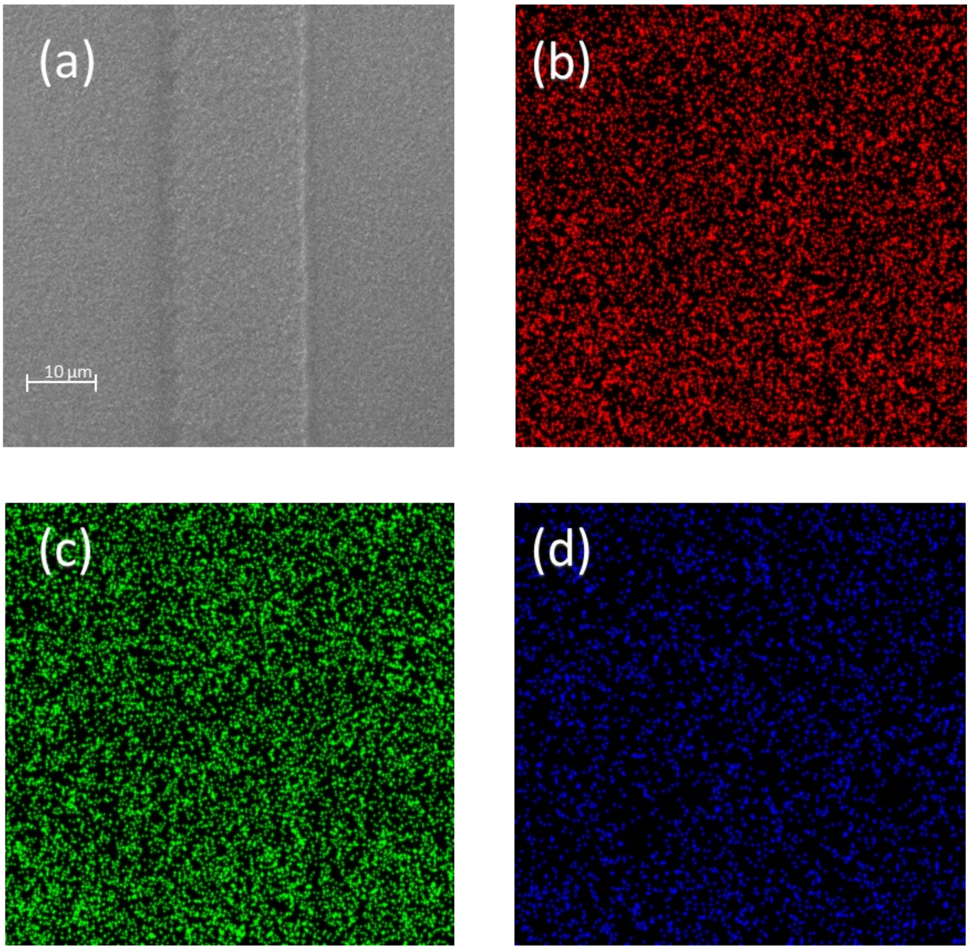

**Figure S2:** (a) SEM images of a pristine and EDS mappings of the same area of showing the distribution of (a) I; (b) Pb; and (c) C elements

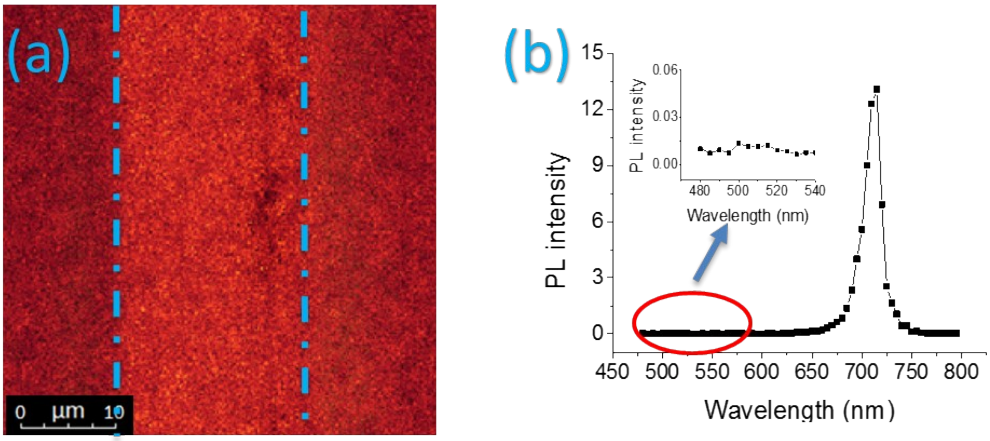

**Figure S3:** (a) Fluorescence image of the pre-moisturized sample with one day recovery recovery from 15 minutes biasing at 0.5 V/µm; and (f) PL spectra of the entire area

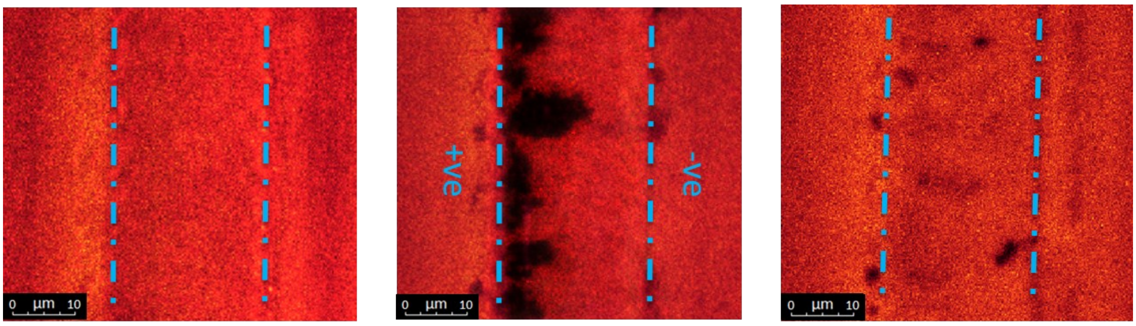

**Figure S4:** Fluorescence images of PMMA encapsulated sample, that (a) before biasing; (b) after 3 min biasing of 0.9 V/um; and (c) after one day recovery

**Table S1**: Fitting values for PL decay traces in Figure 6a measured by TCSPC

| Time (s) | β | τ (ns) | ±Err (ns) |
|---|---|---|---|
| 0 | 0.813 | 16.89 | 0.046 |
| 15 | 0.816 | 17.39 | 0.037 |
| 30 | 0.806 | 17.12 | 0.047 |
| 45 | 0.821 | 17.13 | 0.043 |
| 60 | 0.811 | 17.12 | 0.038 |
| 75 | 0.813 | 17.24 | 0.051 |
| 90 | 0.826 | 17.11 | 0.048 |
| 105 | 0.809 | 17.09 | 0.042 |
| 120 | 0.825 | 17.02 | 0.038 |
| 135 | 0.754 | 13.41 | 0.056 |
| 150 | 0.763 | 11.78 | 0.053 |
| 165 | 0.764 | 10.84 | 0.045 |
| 210 | 0.759 | 10.83 | 0.045 |
| 255 | 0.757 | 10.70 | 0.031 |
| 315 | 0.749 | 10.60 | 0.032 |
| 360 | 0.748 | 10.50 | 0.042 |
| 405 | 0.813 | 10.54 | 0.041 |
| 435 | 0.792 | 12.27 | 0.037 |
| 510 | 0.765 | 13.17 | 0.045 |
| 570 | 0.736 | 13.00 | 0.050 |
| 615 | 0.759 | 13.15 | 0.043 |
| 660 | 0.746 | 13.38 | 0.052 |
| 720 | 0.772 | 13.24 | 0.039 |
| 750 | 0.725 | 13.57 | 0.045 |
| 765 | 0.742 | 12.20 | 0.033 |
| 795 | 0.736 | 12.12 | 0.037 |
| 825 | 0.740 | 11.90 | 0.041 |
| 885 | 0.714 | 11.63 | 0.054 |
| 930 | 0.712 | 11.36 | 0.043 |
| 975 | 0.723 | 11.42 | 0.031 |
| 1020 | 0.736 | 11.33 | 0.036 |

## Reference

1. F. Huang, Y. Dkhissi, W. Huang, M. Xiao, I. Benesperi, S. Rubanov, Y. Zhu, X. Lin, L. Jiang and Y. Zhou, *Nano energy*, 2014, **10**, 10-18.
2. A. Pisoni, J. i. Jaćimović, O. S. Barisic, M. Spina, R. Gaál, L. Forró and E. Horváth, *The journal of physical chemistry letters*, 2014, **5** (14), 2488-2492.
3. J. Qiu, Y. Qiu, K. Yan, M. Zhong, C. Mu, H. Yan and S. Yang, *Nanoscale*, 2013, **5** (8), 3245-3248.
4. J. A. Christians, P. A. Miranda Herrera and P. V. Kamat, *Journal of the American Chemical Society*, 2015, **137** (4), 1530-1538.